stanislav.jelavic@sund.ku.dk

Fate of adsorbed organic compounds during transformation of ferrihydrite: implications for biogenic origin of Precambrian iron formations

S. Jelavić,[1,2*] A. Mitchell[3] and K.K. Sand[1,2,3]

[1]Nano-Science Center, Department of Chemistry, University of Copenhagen, Universitetsparken 5, Copenhagen, Denmark

[2]Section for GeoGenetics, Globe Institute, University of Copenhagen, Øster Voldgade 5-7, Copenhagen, Denmark

[3]University of Aberystwyth, Geography & Earth Sciences, Aberystwyth, UK

[*]Corresponding author: stanislav.jelavic@sund.ku.dk

ABSTRACT

The absence of organic compounds from Precambrian iron formations challenges the hypothesis that they were precipitated by microbial oxidation of Fe (II) to Fe (III). The mineral association of iron formations is a mixture of primary and secondary minerals, where the primary mineral hematite was unlikely precipitated directly in the water column by microbes but rather transformed from a precursor biogenic ferrihydrite. Here we address the fate of the associated organic compounds during mineral transformation. We used dynamic force spectroscopy (DFS) to determine the Gibbs free energy of binding (ΔG_{bu}) between hematite and common molecular terminations found in microbial extracellular polymeric substances (EPS) and biofilms: carboxylic, alcohol and phosphate functional groups. We found that the bond between hematite and alcohol group is approximately 2 times stronger than the bond between hematite-carboxyl and hematite-phosphate groups. To address the fate of the strongly bound polymers during transformation, we transformed synthetic ferrihydrite to hematite in presence of glycerol, which has a high density of alcohol groups, glycerol. The amount of mineral associated glycerol was measured before and after the transformation with thermogravimetric analysis (TGA). We show that the transformation of precursor ferrihydrite to hematite releases glycerol highlighting that at least parts of the organic compounds from initial iron formations were desorbed very early during the process of sedimentation. Our results contribute to understanding of sedimentation of iron formations and open new perspectives in investigation of fate of organic compounds in the Precambrian ocean.

An increasing amount of evidence points toward an active role of microbes in the precipitation of iron formations (IF). The role of anoxygenic phototrophic bacteria in the precipitation of IFs has been speculated since the work of Garrels et al. (Garrels *et al.*, 1973) and since then, many studies looking at the iron (oxyhydr)oxide precipitation by microaerophilic Fe(II)-oxidising bacteria (Nealson, 1982; Emerson & Revsbech, 1994; Chan *et al.*, 2009) such as *Gallionela ferruginea* and *Leptothrix ochracea* or Fe(II)-oxidising phototrophic bacteria (Widdel *et al.*, 1993; Konhauser *et al.*, 2002b; Kappler & Newman, 2004; Kappler *et al.*, 2005; Miot *et al.*, 2009) such as *Rhodobacter ferooxidans* supported a biogenic origin of IF (Søgaard *et al.*, 2000; Konhauser *et al.*, 2002b; Chan *et al.*, 2016). In fact, a mass balance considerations showed that Fe (II)-oxidising phototrophic bacteria could have oxidised all the Fe(II) from the bottom of the Precambrian ocean, leading to its precipitation as iron (oxyhydr)oxide (Konhauser *et al.*, 2002a; Kappler *et al.*, 2005; Hegler *et al.*, 2008). However, a lack of sufficient amount of organic compounds, or their diagenetic or metamorphic products, associated with IF challenges the biogenic origin hypothesis.

Bacteria can induce the precipitation of FeOx in which case the mineral is a product of metabolism (Frankel & Bazylinski, 2003) or they can control the FeOx formation in which case the minerals have a metabolic or functional role, e.g., in the magnetotactic bacteria (Lowenstam, 1981). Currently, our understanding of the Precambrian ocean biogeochemistry indicates that the bacterial oxidation of Fe(II) to Fe(III) occurred through a metabolic pathway. Bacteria use extracellular polymeric substances to facilitate mineral precipitation (Tourney & Ngwenya, 2014; Xiao & Zhao, 2017). In this metabolic pathway bacteria do BLABLA and use their extracellular BLBLA. Microbial extracellular biopolymers are mainly a mixture of polysaccharides, lipids and proteins and contain a range of functional groups, the most common groups being carboxyl (COO(H)), phosphate (PO_4H_x) and alcohol (OH). *Gallionella* have twisted polysaccharide rich stalks that protrude from the cell. When the bacteria oxidises Fe (II) to Fe (III) as a result of its metabolism, the PS stalks scavenge the little soluble Fe (III) species. Sand et al. (Sand *et al.*, 2019) recently showed that such polymers decrease the barriers for FeOx nucleation which explain the observed intimate association between the iron oxides and the bacterial stalks (Chan *et al.*, 2009). When the stalks get encrusted, they are shedded and bacteria form new stalks. The Fe-polymer aggregates would have settled through the water column and deposited on the sea floor as the banded IFs. This mechanism of banded IF deposition implies

that there must be a significant amount of organic compounds present in the initial IFs, prior to carbon breakdown by various microbe-driven processes, or the diagenetic and metamorphic changes. The carbon breakdown is assumed to be of minor importance in Precambrian ocean because of the largely anoxic conditions that prevailed in the water column (Canfield, 1998). However, the degradation of organic compounds would have been promoted by high temperatures and pressures experienced during diagenesis and metamorphism. Siderite has been shown to be a main product of degradation of organic compounds in anoxic BIF microenvironment (Köhler *et al.,* 2013). However, siderite does not occur in all of IFs and does not occur in sufficient amounts to account for the missing microbial mass, still raising questions about the fate of organic compounds in IFs.

Ferrihydrite is the most likely first phase to be precipitated by Fe-oxidising bacteria (Kappler & Newman, 2004) because it is one of the most thermodynamically stable iron phases at the nanoscale (Navrotsky *et al.*, 2008). However, ferrihydrite is a transient phase that readily recrystallizes to more stable, macroscale polymorphs over time (Schwertmann & Cornell, 2000). The transformation from ferrihydrite to hematite is a solid-state process implying that a) there is a phase transition where atoms move locally to attain new structure and b) there is limited long-range diffusion of hydrogen to account for changes in composition between ferrihydrite and hematite. Contrary to dissolution and precipitation processes (e.g., when ferrihydrite transforms to goethite), solid-state transformation does not require a removal (dissolution) of an interface. This indicates that, during a transformation from ferrihydrite to hematite, ferrihydrite-solution and the ferrihydrite-hematite interfaces remain intact suggesting that the binding to organic compounds is not affected. Thus, the transformation of ferrihydrite to hematite in the water column of the Precambrian ocean or in the sediments during diagenesis or metamorphosis should not have to be accompanied by a removal of organic compounds. In contrast, we would expect transformation to other FeOx phases to release any (or parts of) associated microbial organic compounds. Hence, one part of microbially precipitated ferrihydrite in Precambrian ocean would have settled through the water column together with associated organic compounds and would be subsequently diageneticaly and metamorphicaly transformed. However, another part would have been transformed to hematite directly in the water column (Sun *et al.*, 2015) and potentially retain the associated organic compounds. To understand the behaviour of organic compounds during the

transformation from ferrihydrite to hematite, we investigated the energy of binding between hematite and various organic functional groups to identify the strong bond and subsequently, address how it behaves during transformation.

Hematite-organic compound bond strength

To determine the strongest bond between hematite and microbial polymers, we used dynamic force spectroscopy (DFS). We functionalised the AFM tip with common functional groups from biopolymers: we covalently bonded alkyl thiols with carboxylic (COO^-), alcohol (OH), and phosphate (HPO_4^-) head groups to an AFM tip. During the measurements, we allowed the head groups to bind to the hematite surface (Figure 1a) and then measured the forces used to break the bond. The obtained data show an interacting force as a function of distance between the AFM tip and hematite surface and it is called a force curve (Figure 1b). The force curve shows the approach of AFM tip toward the contact with the hematite surface and the subsequent retraction away from the surface. From the force curve, we can determine the rupture force at which the bond between a functional group and a mineral surface breaks. The magnitude of the rupture force increases with the increase of the velocity by which the AFM tip and the hematite surface are pulled apart. Hundreds of force curves were collected for each retracting velocity. From the average rupture forces and their dependence with the loading rate (retraction velocity normalised with the spring constant), we can plot a force spectrum. From the force spectrum, we extract the rupture force at zero external loading, f_{eq}, the distance between the energy at the minimum of the bound state and the energy at the transition to the unbound state, x_t, and the intrinsic rate of unbinding, k_{off} (Table 1). These parameters that describe the energy landscape between an organic functional group and hematite are then used to calculate the Gibbs free energy of binding, ΔG_{bu}, for each ligand-hematite pair using the Friddle multibond approach (Friddle *et al.*, 2012):

$$\Delta G_{bu} = k_B T ln \frac{f_{eq} x_t}{k_B T} + f_{eq} x_t + k_B T,$$

where k_B represents the Boltzmann constant (1.380649×10^{-23} JK^{-1}) and T, the temperature (K).

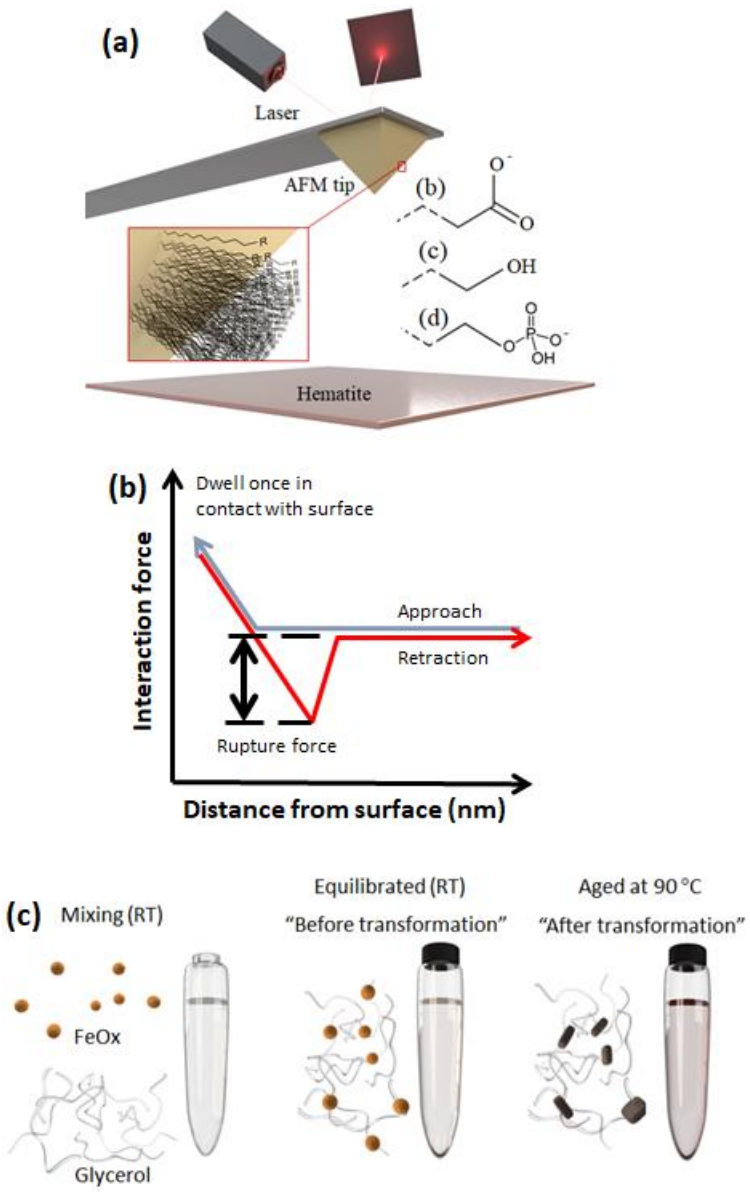

Figure 1. a) Schematics of the dynamic force spectroscopy experiment: self-assembled monolayers containing carboxyl, alcohol and phosphate headgroups were covalently bonded to AFM tip and brought in contact with the hematite surface. b) Tracking the movements of the AFM tip with a laser allows us to reconstruct the forces between the AFM tip and hematite surface in a force. C) In transformation experiments, ferrihydrite and glycerol were mixed at room temperature and left to equilibrate overnight. One sample was then taken for measurements (equilibrium sample) and the rest was placed in the oven at 90 ºC until the transformation to hematite was complete (aged sample).

Table 1. Binding parameters.

	Hematite – HPO_4^-	Hematite – COO^-	Hematite – OH
x_t (Å)	0.4 ± 0.3	0.40 ± 0.04	0.10 ± 0.04
k_{off} (s^{-1})	241 ± 352	1934 ± 570	1351 ± 1360
f_{eq} (pN)	104 ± 18	83 ± 8	597 ± 18

* uncertainty expressed as a standard deviation

The bond strength between organic compounds and mineral surfaces depends on the composition of the surrounding solution, in particular the pH and the ionic strength. We have conducted our DFS experiments at pH=5.5 and at 10 mM NaCl. Our pH is for ~1 unit lower than the current estimates for Precambrian seawater (Halevy & Bachan, 2017; Krissansen-Totton *et al.*, 2018). However, we chose it because the hematite {0001} surface potential is mostly neutral and the zeta potential is slightly positive (Chatman *et al.*, 2013; Lützenkirchen *et al.*, 2013; Wang *et al.*, 2016), which resembles the surface properties of particulate hematite at circumneutral conditions. We used the solution concentration of 10 mM instead of much higher concentration typical for seawater. We chose not to work with solution similar to seawater because we wanted to avoid issues with divalent cations and high activities.

We found that the binding between hematite and the OH group (ΔG_{bu}=2.8±0.7 kT) is approximately 2 times stronger than the binding to COO^- (ΔG_{bu}=1.6±0.2 kT) and HPO_4^- groups (ΔG_{bu}=1.6±0.6 kT) (Fig. 2). These values are comparable to the ΔG_{bu} between goethite and COO^- (1.0±0.6 kT), and goethite and PO_3^- (1.6±0.9 kT) measured at pH=6 (Newcomb *et al.*, 2017). The difference between the values of ΔG_{bu} in our and Newcomb et al., most likely arises from a sligthly different pH at which the measurements were done and the variations in the AFM tip geometry that affects the value of f_{eq}. Our results show that microbial biopolymers rich in alcohol functional groups bind stronger to hematite than the biopolymers rich in acidic groups such as COO^- and HPO_4^-. The weaker binding of hematite to the acid compared to alcohol functional group also implies that, irrespective of the transformation pathway from ferrihydrite to hematite, biopolymers rich in acidic groups adsorb less strongly or desorb more easily from hematite than the one rich in alcohol group.

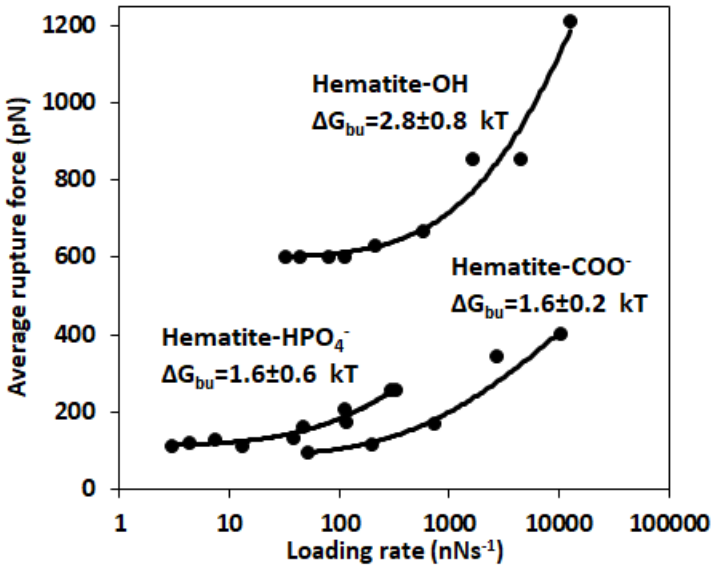

Figure 2. Multibond fit to the dynamic force spectra between hematite surface and alkyl thiol SAMs with alcohol (OH), phosphate (HPO_4^-) and carboxyl (COO^-) head groups. ΔG_{bu} were calculated using the Friddle approach. The uncertainty represents the error propagated from the multibond fit to a spectrum. Loading rate is a nominal retraction velocity (nms^{-1}) multiplied with the spring constant of the cantilever ($nNnm^{-1}$).

The ferrihydrite to hematite transformation pathway

Having identified hematite-OH containing biopolymer as the strongest bond, thus the one least likely to break during the transformation, we transformed ferrihydrite to hematite in presence of glycerol (CH_2**OH**-CH**OH**-CH_2**OH**) (Supplementary Information file). We chose glycerol to isolate the effect of the bond strength on the magnitude of desorption of organic compounds, without additional interactions (e.g. hydrophobic effect (Van Oss *et al.*, 1986; Li & Walker, 2011)) or phenomena (e.g. biopolymer conformation variations close to a surface (Kiriy *et al.*, 2002; Pastré *et al.*, 2003)) accompanying large and complex OH-containing polymers. Glycerol has a relatively high density of OH groups and it is miscible with water, which is an advantage compared to polysaccharides readily used as a model for extracellular polymeric substances. In addition, in presence of glycerol, ferrihydrite transformed directly to hematite (Figure S3, Supplementary Information File), without goethite intermediate indicating a solid-state transformation. The solid-state transformation pathway was important because in that way we avoided desorption of glycerol during the ferrihydrite dissolution and the subsequent readsorption of glycerol to newly formed goethite and/or hematite.

The transformation pathway was different when ferrihydrite was transformed in 0.5 M NaCl (saline) or in saline with glycerol (Figure S2 and S3, Supplementary Information File). In saline, ferrihydrite transformed directly to hematite after 17 h and goethite started to crystallise after 43 hours. After 96 hours of transformation, the final product consisted of a mixture of hematite and goethite. In saline containing glycerol, the only detected product of ferrihydrite transformation was hematite. The transformation to hematite started earlier than in the pure saline solution suggestion higher transformation rate of ferrihydrite in presence of glycerol.

The transformation is accompanied by a release of glycerol

To estimate the amount of glycerol adsorbed to ferrihydrite before transformation (equilibrated in glycerol solution) and to hematite after transformation (aged in glycerol solution), we measured the weight loss of ferrihydrite and hematite, with and without glycerol, using the thermogravimetric analysis (Figure 3, Supplementary Information file for details). The weight loss <125 ºC accounts for the loss of adsorbed water. It is higher for ferrihydrite-glycerol complex than for hematite-glycerol complex because ferrihydrite is more hydrated than hematite. On the other hand, the weight loss between 125-700 ºC can be ascribed to the combined loss of the tightly bound water and glycerol. The content of tightly bound water is also higher in ferrihydrite than in hematite (Hiemstra and Van Riemsdijk, 2009; Cornell and Schwertmann, 2004). However, the comparison between the weight losses in the range 125-700 ºC of ferrihydrite equilibrated without the presence of glycerol (blank- 4.7%; Table 2) and the ferrihydrite equilibrated in the presence of glycerol (glycerol- 5.4%; Table 2) shows that the tightly bound water can account for only 87 % of the weight loss, indicating that the difference to the 100% is the loss of glycerol. In general, the samples equilibrated or aged in presence of glycerol have lost more weight than the samples equilibrated or aged in absence of glycerol. Among the glycerol containing samples, ferrihydrite lost more weight compared to hematite indicating a higher content of glycerol on ferrihydrite than on hematite. This goes in line with previous observations that the ferrihydrite forms stronger bonds with alginate, a model for an extracelullar polysaccharide, than hematite (Sand *et al.*, 2019). Thus, hematite produced by aging ferrihydrite in a glycerol solution contains less glycerol than the original ferrihydrite that was only equilibrated with glycerol overnight.

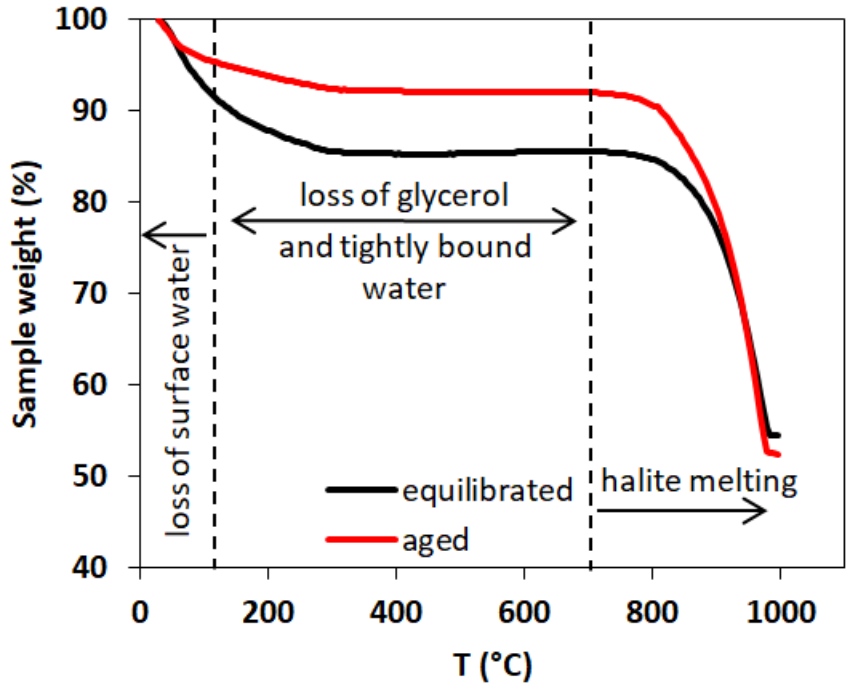

Figure 3. Comparison of thermogravimetric curves of precursor ferrihydrite mixed with glycerol (equilibrium-black curve) and resulting hematite with glycerol (aged- red curve). The smaller mass loss in the region 125-700 °C (dashed vertical lines) for the aged sample compared to the equilibrium sample suggests loss bigger particle sizes with less tightly bound water and loss of glycerol during the transformation.

Table 2. Mass losses during the TGA analysis in the region <125 °C corresponding to the loss of loosely adsorbed or surface water and in the region 125-700 °C that corresponds to loss of both tightly bound water and glycerol.

Sample		**weight % loss**	
		<125 °C	**125-700 °C**
Glycerol	**equilibrated**	**8.9**	**5.4**
	aged	**4.8**	**3.2**
Blank	**equilibrated**	**9.8**	**4.7**
	aged	**n.a.***	**n.a.**

* transformation yielded both goethite and hematite making comparison impossible

The reason for the loss of the glycerol during the transformation can be smaller specific surface area (SSA) of the produced hematite (Figure S4, Suuplementary Information file) or the lower affinity of hematite to organic molecules compared to ferrihydrite (Sand *et al.*, 2019). From TEM

images, we estimated the specific surface area of the precursor ferrihydrite, assuming its ideal spherical shape, and of produced hematite by taking the average of the particle dimensions (TEM). The SSA of precursor ferrihydrite is between 374-790 m^2g^{-1} and of resulting hematite between 10-46 m^2g^{-1}. Thus, the possible decrease in the SSA is anything between 9-70 times which alone is certainly possible to explain the decrease in glycerol content after transformation. However, the loss must be augmented by the decrease in binding affinity of organic compounds between ferrihydrite and hematite as well. Both the decrease of SSA and the decrease of the affinity are likely explanations for our observations and both scenarios are likely to have contributed to the loss of organic matter during the formation of BIFs. At the moment, we are unable to discern which of those scenarios have contributed more to the organic matter recycling in the Precambrian oceans. To approach this question quantitatively, we have to be able to precisely measure the amount of adsorbed glycerol before and after the transformation. Currently, the presence of tightly bound water in the transformation product makes difficult to do so and we are currently working on elucidating this issue.

We have demonstrated that glycerol, the molecule with a high Gibbs free energy of binding to hematite, desorbs during the transformation of ferrihydrite to hematite. The partial loss of glycerol during the transformation contributes to efforts in explaining the absence of organics from BIFs. We propose that a significant amount of organic matter has been desorbed early in the process of FeOx sedimentation as a consequence of transformation of precursor ferrihydrite to more stable hematite in oxic conditions. This loss in organic compounds is probably further enhanced by the grain coarsening of hematite during diagenetic and metamorphic processes or reductive transformation of Fe(III) phases to siderite and magnetite. In addition, these conclusions suggest that the use of siderite as a proxy for Archean seawater biomass should be considered as very conservative and that the biomass was higher than what would siderite rich iron formations imply.

ACKNOWLEDGMENTS

We thank Heloisa N. Bordallo for access to TGA instrument (Carlsbergfondets, grant no. 2013_01_0589). KKS and ACM are grateful for funding from the European Union's Horizon 2020 Research and Innovation Programme under Marie Skłodowska-Curie Grant Agreement No 663830 and the Welsh Government and Higher Education Funding Council for Wales through the Sêr Cymru National Research Network for Low Carbon, Energy and Environment. KKS is grateful for funding from the Danish Council for Independent Research Sapere Aude Programs (0602-02654B).

REFERENCES:

Canfield DE (1998) A new model for Proterozoic ocean chemistry. *Nature* **396**, 450.

Chan CS, Fakra SC, Edwards DC, Emerson D, Banfield JF (2009) Iron oxyhydroxide mineralization on microbial extracellular polysaccharides. *Geochimica Et Cosmochimica Acta* **73**, 3807–3818.

Chan CS, McAllister SM, Leavitt AH, Glazer BT, Krepski ST, Emerson D (2016) The Architecture of Iron Microbial Mats Reflects the Adaptation of Chemolithotrophic Iron Oxidation in Freshwater and Marine Environments. *Frontiers in Microbiology* **7**.

Chatman S, Zarzycki P, Rosso KM (2013) Surface potentials of (001), (012), (113) hematite (α-Fe2O3) crystal faces in aqueous solution. *Physical Chemistry Chemical Physics* **15**, 13911–13921.

Emerson D, Revsbech NP (1994) Investigation of an Iron-Oxidizing Microbial Mat Community Located near Aarhus, Denmark: Laboratory Studies. *Applied and Environmental Microbiology* **60**, 4032–4038.

Frankel RB, Bazylinski DA (2003) Biologically Induced Mineralization by Bacteria. *Reviews in Mineralogy and Geochemistry* **54**, 95–114.

Friddle RW, Noy A, Yoreo JJD (2012) Interpreting the widespread nonlinear force spectra of intermolecular bonds. *Proceedings of the National Academy of Sciences* **109**, 13573–13578.

Garrels RM, Perry EA, Mackenzie FT (1973) Genesis of Precambrian Iron-Formations and the Development of Atmospheric Oxygen. *Economic Geology* **68**, 1173–1179.

Halevy I, Bachan A (2017) The geologic history of seawater pH. *Science* **355**, 1069–1071.

Hegler F, Posth NR, Jiang J, Kappler A (2008) Physiology of phototrophic iron(II)-oxidizing bacteria: implications for modern and ancient environments. *FEMS Microbiology Ecology* **66**, 250–260.

Kappler A, Newman DK (2004) Formation of Fe(III)-minerals by Fe(II)-oxidizing photoautotrophic bacteria 11Associate editor: L. G. Benning. *Geochimica et Cosmochimica Acta* **68**, 1217–1226.

Kappler A, Pasquero C, Konhauser KO, Newman DK (2005) Deposition of banded iron formations by anoxygenic phototrophic Fe(II)-oxidizing bacteria. *Geology* **33**, 865–868.

Kiriy A, Gorodyska G, Minko S, Jaeger W, Štěpánek P, Stamm M (2002) Cascade of Coil-Globule Conformational Transitions of Single Flexible Polyelectrolyte Molecules in Poor Solvent. *Journal of the American Chemical Society* **124**, 13454–13462.

Köhler I, Konhauser KO, Papineau D, Bekker A, Kappler A (2013) Biological carbon precursor to diagenetic siderite with spherical structures in iron formations. *Nature Communications* **4**, 1–7.

Konhauser K, Hamade T, Raiswell R, Canfield DE (2002a) Could bacteria have formed the Precambrian banded iron formations? *Geology* **30**.

Konhauser KO, Hamade T, Raiswell R, Morris RC, Ferris FG, Southam G, Canfield DE (2002b) Could bacteria have formed the Precambrian banded iron formations? *Geology* **30**, 1079–1082.

Krissansen-Totton J, Arney GN, Catling DC (2018) Constraining the climate and ocean pH of the early Earth with a geological carbon cycle model. *Proceedings of the National Academy of Sciences* **115**, 4105–4110.

Li ITS, Walker GC (2011) Signature of hydrophobic hydration in a single polymer. *Proceedings of the National Academy of Sciences* **108**, 16527.

Lowenstam HA (1981) Minerals formed by organisms. *Science* **211**, 1126–1131.

Lützenkirchen J, Preočanin T, Stipić F, Heberling F, Rosenqvist J, Kallay N (2013) Surface potential at the hematite (001) crystal plane in aqueous environments and the effects of prolonged aging in water. *Geochimica et Cosmochimica Acta* **120**, 479–486.

Miot J, Benzerara K, Morin G, Kappler A, Bernard S, Obst M, Férard C, Skouri-Panet F, Guigner J-M, Posth N, Galvez M, Brown GE, Guyot F (2009) Iron biomineralization by anaerobic neutrophilic iron-oxidizing bacteria. *Geochimica et Cosmochimica Acta* **73**, 696–711.

Navrotsky A, Mazeina L, Majzlan J (2008) Size-Driven Structural and Thermodynamic Complexity in Iron Oxides. *Science* **319**, 1635–1638.

Nealson KH (1982) Microbiological Oxidation and Reduction of Iron. In: *Mineral Deposits and the Evolution of the Biosphere*, Dahlem Workshop Report (eds. Holland HD, Schidlowski M). Springer Berlin Heidelberg, pp. 51–65.

Newcomb CJ, Qafoku NP, Grate JW, Bailey VL, Yoreo JJD (2017) Developing a molecular picture of soil organic matter–mineral interactions by quantifying organo–mineral binding. *Nature Communications* **8**, 396.

Pastré D, Piétrement O, Fusil S, Landousy F, Jeusset J, David M-O, Hamon L, Le Cam E, Zozime A (2003) Adsorption of DNA to Mica Mediated by Divalent Counterions: A Theoretical and Experimental Study. *Biophysical Journal* **85**, 2507–2518.

Sand KK, Jelavic S, Dobberschütz S, Ashby PD, Marshall MJ, Dideriksen K, Stipp SLS, Kerisit SN, Friddle RW, DeYoreo JJ (2019) Mechanistic Insight into Biopolymer Induced Iron Oxide Mineralization Through Quantification of Molecular Bonding.

Schwertmann U, Cornell RM (2000) Ferrihydrite. In: *Iron Oxides in the Laboratory*. John Wiley & Sons, Ltd, Weinheim, Federal Republic of Germany, pp. 103–112.

Søgaard EG, Medenwaldt R, Abraham-Peskir JV (2000) Conditions and rates of biotic and abiotic iron precipitation in selected Danish freshwater plants and microscopic analysis of precipitate morphology. *Water Research* **34**, 2675–2682.

Sun S, Konhauser KO, Kappler A, Li Y-L (2015) Primary hematite in Neoarchean to Paleoproterozoic oceans. *GSA Bulletin* **127**, 850–861.

Tourney J, Ngwenya BT (2014) The role of bacterial extracellular polymeric substances in geomicrobiology. *Chemical Geology* **386**, 115–132.

Van Oss CJ, Good RJ, Chaudhury MK (1986) The role of van der Waals forces and hydrogen bonds in "hydrophobic interactions" between biopolymers and low energy surfaces. *Journal of Colloid and Interface Science* **111**, 378–390.

Wang Y, Persson P, Michel FM, Brown GE (2016) Comparison of isoelectric points of single-crystal and polycrystalline α-Al2O3 and α-Fe2O3 surfaces. *American Mineralogist* **101**, 2248–2259.

Widdel F, Schnell S, Heising S, Ehrenreich A, Assmus B, Schink B (1993) Ferrous iron oxidation by anoxygenic phototrophic bacteria. *Nature* **362**, 834–836.

Xiao Y, Zhao F (2017) Electrochemical roles of extracellular polymeric substances in biofilms. *Current Opinion in Electrochemistry* **4**, 206–211.